


# Phytochemical library screening reveals betulinic acid as a novel Skp2-SCF E3 ligase inhibitor in non-small cell lung cancer

Dan-Hua He<sup>1,2</sup> | Yu-Fei Chen<sup>1,2</sup> | Yi-Le Zhou<sup>1</sup> | Shi-Bing Zhang<sup>1</sup> | Ming Hong<sup>1</sup> | Xianjun Yu<sup>5</sup> | Su-Fen Wei<sup>1</sup> | Xiang-Zhen Fan<sup>1</sup> | Si-Yi Li<sup>1</sup> | Qi Wang<sup>1</sup> | Yongzhi Lu<sup>3,4</sup> | Yong-Qiang Liu<sup>1,2</sup> 

<sup>1</sup>Institute of Clinical Pharmacology, Science and Technology Innovation Center, Guangzhou University of Chinese Medicine, Guangzhou, China

<sup>2</sup>Research Center of Chinese Herbal Resources Science and Engineering, School of Pharmaceutical Sciences, Key Laboratory of Chinese Medicinal Resource from Lingnan, Ministry of Education, Guangzhou University of Chinese Medicine, Guangzhou, China

<sup>3</sup>Guangzhou Regenerative Medicine and Health Guangdong Laboratory, Guangzhou, China

<sup>4</sup>State Key Laboratory of Respiratory Disease, Guangzhou Institutes of Biomedicine and Health, Chinese Academy of Sciences, Guangzhou, China

<sup>5</sup>Laboratory of Inflammation and Molecular Pharmacology, School of Basic Medical Sciences and Biomedical Research Institute, Hubei University of Medicine, Shiyan, China

## Correspondence

Yong-Qiang Liu, Guangzhou University of Chinese Medicine, 232 Waihuan East Road, Guangzhou 510006, China.  
Email: liuyq@gzucm.edu.cn

Yongzhi Lu, Guangzhou Institutes of Biomedicine and Health, 190 Kaiyuan Avenue, Guangzhou 510005, China.  
Email: lu\_yongzhi@gibh.ac.cn

## Funding information

Project of south medicine innovation team in modern agricultural industry technology system of Guangdong Province, Grant/Award Number: 2020KJ148; National Natural Science Foundation of China, Grant/Award Number: 81802776 and 82004161; Guangzhou Science Technology and Innovation Commission Technology Research Projects, Grant/Award Number: 201805010005

## Abstract

Skp2 is overexpressed in multiple cancers and plays a critical role in tumor development through ubiquitin/proteasome-dependent degradation of its substrate proteins. Drugs targeting Skp2 have exhibited promising anticancer activity. Here, we identified a plant-derived Skp2 inhibitor, betulinic acid (BA), via high-throughput structure-based virtual screening of a phytochemical library. BA significantly inhibited the proliferation and migration of non-small cell lung cancer (NSCLC) through targeting Skp2-SCF E3 ligase both in vitro and in vivo. Mechanistically, BA binding to Skp2, especially forming H-bonds with residue Lys145, decreases its stability by disrupting Skp1-Skp2 interactions, thereby inhibiting the Skp2-SCF E3 ligase and promoting the accumulation of its substrates; that is, E-cadherin and p27. In both subcutaneous and orthotopic xenografts, BA significantly inhibited the proliferation and metastasis of NSCLC through targeting Skp2-SCF E3 ligase and upregulating p27 and E-cadherin protein levels. Taken together, BA can be considered a valuable therapeutic candidate to inhibit metastasis of NSCLC.

## KEYWORDS

betulinic acid, E-cadherin, metastasis, NSCLC, Skp2

**Abbreviations:** BA, betulinic acid; CDDP, cisplatin; CHX, cycloheximide; EMT, epithelial-mesenchymal transition; H&E, hematoxylin and eosin; NSCLC, non-small cell lung cancer; SCF, Skp1-Cullin1-F-box protein.

This is an open access article under the terms of the Creative Commons Attribution-NonCommercial-NoDerivs License, which permits use and distribution in any medium, provided the original work is properly cited, the use is non-commercial and no modifications or adaptations are made.

© 2021 The Authors. *Cancer Science* published by John Wiley & Sons Australia, Ltd on behalf of Japanese Cancer Association.

## 1 | INTRODUCTION

Lung cancer is the leading cause of cancer-related mortality worldwide. Most non-small cell lung cancer (NSCLC) patients succumb to the disease due to drug resistance and cancer metastasis.<sup>1</sup> Targeted therapies have shown clinical benefits and promising prospects in NSCLC. However, few anticancer drugs that target tumor metastases have been developed.<sup>2</sup> Therefore, novel drugs that suppress NSCLC metastasis are urgently needed.

It is widely accepted that the Skp1-Cullin1-F-box protein (SCF) complex plays critical roles in tumorigenesis and cancer development by regulating protein degradation. Skp2, an F-box protein of the SCF complex, is overexpressed in various human cancers and promotes tumor development.<sup>3</sup> The Skp2-SCF complex participates in cancer cell proliferation and migration through ubiquitin-dependent degradation of p27 and E-cadherin.<sup>4,5</sup> Components of SCF complex, including Cullin1, Skp1, and certain F-box proteins, have demonstrated to be promising therapeutic targets in cancer treatments.<sup>6,7</sup> In particular, several Skp2-targeting compounds, such as SMIP004, compound A, compound #25, and C1/2, were found to exhibit significant anticancer effects,<sup>8-11</sup> suggesting that Skp2 is a potential therapeutic target for NSCLC.

Accumulating evidence indicates that numerous phytochemicals exhibit promising antitumor activities.<sup>12</sup> Hence, these are considered suitable candidate drugs for novel anticancer therapies.<sup>13</sup> In this study, we aimed to discover plant-derived inhibitors specific for Skp2. High-throughput structure-based virtual screening was used to screen a phytochemical library that had been previously used for other purposes.<sup>7</sup> All the phytochemicals of the library were collected from published literature. We identified a potent Skp2 inhibitor, betulinic acid (BA), which binds to Skp2 by forming H-bonds with residue Lys145 and leads to Skp2 downregulation, p27 and E-cadherin accumulation, and a decrease of migratory potential of NSCLC. Thus, our study screened a phytochemical library to identify Skp2 inhibitors, and then provided evidence that BA can be used as an antimetastatic agent that targets Skp2-SCF E3 ligase in NSCLC.

## 2 | MATERIALS AND METHODS

### 2.1 | Reagents and antibodies

Betulinic acid and cycloheximide (CHX) were purchased from Meilun Biotechnology. SZL-P1-41 (compound #25) was purchased from MedChemExpress. Procyanidin B1 was purchased from Sichuan Victory Biotechnology. Hesperidin and Camptothecin were purchased from Aladdin Chemistry. TGF- $\beta$  was purchased from PeproTech. Antibodies against Skp2 (#2652), p27 (#3688), E-cadherin (#14472), and GAPDH (#2118) were obtained from Cell Signaling Technology; antibodies against N-cadherin (ab76011), Vimentin (ab92547), Twist (ab175430), Slug (ab106077), and Snail (ab216347) were purchased from Abcam; antibody against Skp1 (GTX106675) was purchased from GeneTex; antibody against Flag

(F1804) was purchased from Sigma; antibody against HA (A02040) Myc (A02060) was purchased from Abbkine. All secondary antibodies (HRP-conjugated anti-mouse IgG and anti-rabbit IgG) were purchased from Cell Signaling Technology.

### 2.2 | Cell culture and treatment

The human lung cancer cell lines A549 and H1299, the mouse Lewis lung carcinoma cell line (LLC), and human kidney cell line 293T within four passages were purchased from the ATCC, A549-luciferase cell line was a gift from Professor Guang-Biao Zhou from the State Key Laboratory of Molecular Oncology, National Cancer Center. The A549, LLC, and 293T cells were cultured in DMEM and H1299 cells were cultured in RPMI-1640 medium (Hyclone), supplemented with 10% FBS (Hyclone), penicillin (100 IU/mL), and streptomycin (100  $\mu$ g/mL) (Invitrogen) in a humidified incubator containing 5% CO<sub>2</sub> at 37°C.

### 2.3 | Cell viability assay

The H1299, A549, and LLC cells were plated in 96-well plates at  $4 \times 10^3$  cells/well and treated with BA at indicated concentrations for 24 hours or 48 hours. After treatment, the cells were incubated with 10  $\mu$ L 5 mg/mL MTT solution and incubated for an additional 4 hours, then the MTT formazan crystals were dissolved in DMSO (100  $\mu$ L/well) and the absorbance at 490 nm was measured. The assay was performed at least three times.

### 2.4 | Wound-healing and transwell assay

For wound-healing assay, cells ( $4 \times 10^5$ /well) were plated in 6-well plates overnight. Wounds were made in the cell monolayer by micropipette tip and treated with or without BA for 24 hours. Then, the images of wounds were obtained using an inverted microscope. For the transwell invasion assay, cells were plated in the upper chamber of transwell inserts (6.5 mm diameter and 8  $\mu$ m pore size; Corning) that were precoated with Matrigel (Corning) for 4 hours; cells in the upper chamber were cultured in serum-free medium, while the lower chamber was filled with 10% FBS medium as a chemoattractant. After BA treatment for 24 hours, cells in the upper chamber were removed using a cotton swab, and cells in the lower chamber were fixed with methanol, stained with .1% crystal violet, photographed by microscopy, and enumerated by counting three random fields per well. All assays were repeated three times.

### 2.5 | Sphere formation assay

The sphere formation in non-adherent conditions was performed as described previously;<sup>14</sup> briefly, dispersed cells were cultured in serum-free DMEM/F-12 media (Hyclone) supplemented with B27

(1:100, Thermo Fisher Scientific), EGF (20 ng/mL, Sino Biological), FGF (10 ng/mL, Sino Biological), and heparin (5 µg/mL, StemCell Technologies) in ultra-low attachment cell culture plates and treated with DMSO or BA. Tumor spheres were photographed and counted from at least three independent fields for each well. Three-dimensional Matrigel cultures were carried out as previously described;<sup>15</sup> briefly, a total of 100 µL mixture (50 µL cold cell suspension: 50 µL cold Matrigel) was prepared and pipetted into the bottom rim of 12-well plates. Then low-serum (1% FBS) media with or without BA was added to the middle of each well. For the above experiments, the medium was refreshed every 3 days.

## 2.6 | Western blotting

Cells were treated with DMSO or BA for indicated time points, total protein was harvested, and protein concentrations were detected using the BCA Kit (Beyotime). The protein was subjected to SDS-PAGE and transferred to PVDF membranes. These membranes were incubated with indicated antibodies and detected by ChemiDoc XRS system with Quantity One software (Bio-Rad); the images were analyzed by ImageJ software (NIH). Experiments were performed in triplicate.

## 2.7 | Phytochemical library and high-throughput virtual screening

The phytochemical library contains 841 reported plant-derived compounds, including flavonoids, terpenoids, phenolics, tannins, alkaloids, stilbenes, curcuminoids, and glycosides. The three-dimensional structure models of the compounds were prepared as previously described.<sup>7</sup> Crystal structure of Skp2 (PDB, 2AST) was used as the receptor in the molecular docking. Receptor and the compound ligands were prepared using AutoDock Tools<sup>16</sup> and OpenBabel,<sup>17</sup> respectively. The high-throughput molecular docking was carried out using Autodock Vina.<sup>18</sup> The parameters exhaustiveness and num\_modes were set as 50 and 100, respectively. Then, 4 compounds out of the 24 top hits (binding affinity energy < -7.1 kcal/mol) were selected for further analysis (Table S1).

## 2.8 | Cellular thermal shift assay

A cellular thermal shift assay (CETSA) was performed as described previously.<sup>19</sup> Briefly, cells cultured in 10-cm dishes were treated with DMSO or BA for 3 hours. After treatment, cells were harvested and the cell suspensions in PBS were distributed into six PCR tubes and heated to indicated temperatures (42, 46, 50, 54, and 58°C) for 3 minutes. Then the tubes were incubated at room temperature for 3 minutes followed by three repeated freeze-thaw cycles of liquid nitrogen. Subsequently, the cell lysates were centrifuged at 20 000 g at 4°C for 20 minutes, the supernatant was collected for further experiments.

## 2.9 | Co-immunoprecipitation

Co-immunoprecipitation (co-IP) was performed as described previously.<sup>20</sup> Briefly, 293T cells were transfected with HA-tagged Skp2 and Flag-tagged Skp1 using a Calcium Phosphate Cell Transfection Kit (Beyotime). After 48 hours of transfection, cells were cultured with or without BA for 4 hours and lysed with co-IP lysis buffer (137 mmol L<sup>-1</sup> NaCl, 2 mmol L<sup>-1</sup> EDTA, 40 mmol L<sup>-1</sup> Tris-HCl (pH 7.4), 1% NP-40) at 4°C for 30 minutes under gentle rotation. The lysates were centrifuged at 14 000 g, 4°C for 15 minutes. Then the protein concentrations of supernatants were detected by BCA protein assay kit (Beyotime). Equal amounts of the supernatants (50 µg) were aliquoted as "input" samples. For the co-IP assay, 500 µg of the remaining supernatants were incubated with indicated antibodies overnight and then incubated with protein A/G agarose beads (Beyotime) at 4°C for an additional 4 hours. The beads were washed using co-IP lysis buffer and boiled with SDS-PAGE loading buffer. For western blotting, 5 µg proteins of "input" were used to examine the expression levels of interested proteins.

## 2.10 | Skp2 overexpressing stable cell line

To establish Skp2 stably overexpressing cell lines, the human Skp2 cDNA was cloned into the lentiviral expression vector pSin-EF2-puro. 293T cells were transfected with the lentiviral expression vector and packaging vectors using a Calcium Phosphate Cell Transfection Kit. Then lentivirus was harvested to infect H1299 and A549 cells. NSCLC were incubated with medium containing puromycin (5 µg/mL) to generate cells stably overexpressing Skp2.

## 2.11 | In vivo ubiquitination assay

293T cells were transfected with the indicated plasmids, including Skp2, E-cadherin/p27, and HA-tagged ubiquitin, using a Calcium Phosphate Cell Transfection Kit (Beyotime). After 48 hours of transfection, cells were cultured with or without BA for 24 hours and treated with MG132 for an additional 6 hours. Cells were lysed with co-IP lysis buffer containing 10 mmol L<sup>-1</sup> N-ethylmaleimide; the cellular extracts were immunoprecipitated overnight with anti-E-cadherin or anti-p27 antibodies and then subjected to western blotting.

## 2.12 | Animal experiments

All animal studies were approved by and were performed according to the guidelines of the Animal Ethics Committee of Guangzhou University of Chinese Medicine (authorization number 20191112005). All the mice were purchased from Guangdong Medical Laboratory Animal Center. For the spontaneous metastasis mouse model, LLC (1 × 10<sup>6</sup>) cells were injected subcutaneously

into C57BL/6 mice (male, 6 weeks). Once the tumors reach approximately 80 mm<sup>3</sup>, animals were randomly divided into three groups (n = 10 per group): a vehicle control group (solvent: 10% DMSO, 70% cremophor/ethanol (3:1), and 20% saline); and BA treatment groups (i.p., 50 mg/kg and 75 mg/kg). The tumor volumes were measured and calculated as (length × width<sup>2</sup>)/2. After 21 days of treatment, all mice were killed using CO<sub>2</sub> to determine the number of tumor colonies in the lung tissue. For the experimental metastasis mouse model, LLC (1 × 10<sup>6</sup>) cells or A549-luciferase cells (5 × 10<sup>6</sup>) in 100 μL PBS were intravenously injected into C57BL/6 or BALB/c nude mice (male, 6 weeks) via the tail vein, respectively. After 7 days of injection, the mice were randomly divided into three or four groups and administrated with vehicle, BA, or cisplatin (3 mg/kg). For survival assessment, the animals were monitored for 60 days until being killed using CO<sub>2</sub>. The distribution of survival percentages per treatment group was estimated using the Kaplan–Meier method. To assess the effect of BA on tumor growth, *in vivo* bioluminescence imaging of living nude mice anesthetized with isoflurane was performed to accurately visualize the volume of tumors using a Berthold NightOWL LB 983 Imaging System.

## 2.13 | H&E staining and immunohistochemistry

Tissue samples fixed in 4% paraformaldehyde were sequentially dehydrated in a graded alcohol series (70%, 85%, 95%, and 100%). They were then transferred to xylene and embedded in paraffin; the tissues were sectioned to 4-μm thickness for further study. For histological examination, sections were stained with H&E to distinguish tumor metastatic foci from normal tissues. For immunohistochemistry (IHC), the tissue sections were deparaffinized and then preincubated using 10% normal goat serum, followed by incubation with primary antibody at 4°C overnight and the appropriate secondary

antibody for 2 hours at room temperature. Protein expression was then evaluated using an IHC kit (Solarbio).

## 2.14 | Statistical analysis

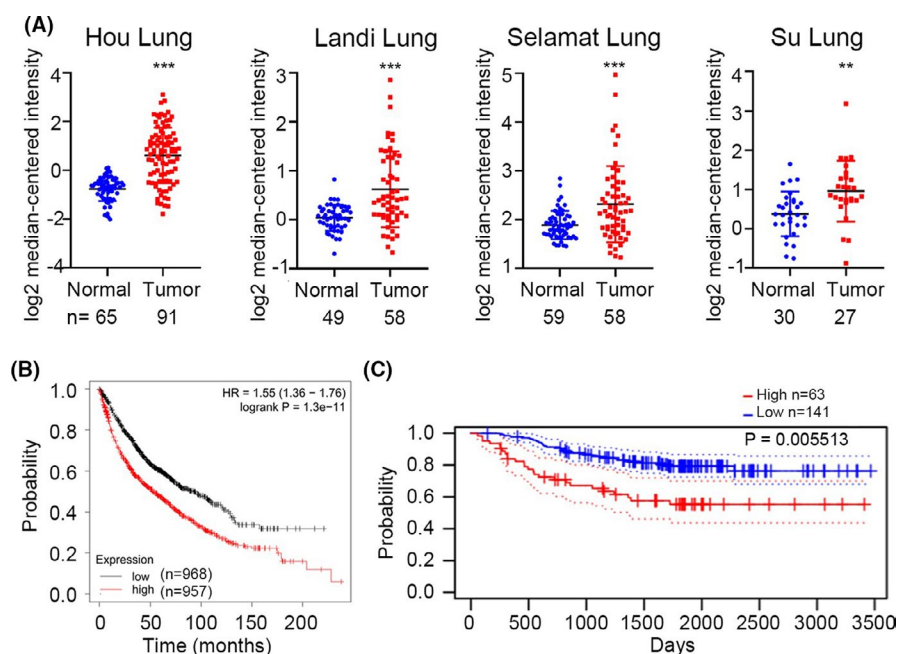
The data are presented as mean ± SEM unless noted otherwise. All statistical analyses were performed using GraphPad Prism 8.0.1 (GraphPad Software). Statistically significant differences between two means were evaluated by unpaired Student's *t* test; the multiple comparisons were done by ANOVA followed by post hoc test. Survival curves were analyzed using GraphPad Prism 8.0.1. *P*-values less than .05 were considered statistically significant. Statistical significance was defined as \**P* < .05, \*\**P* < .01, and \*\*\**P* < .001.

## 3 | RESULTS

### 3.1 | Identification of Skp2 inhibitors by high-throughput structure-based virtual screening

Ample evidence has demonstrated that Skp2 plays an important role in cancer progression. First, we analyzed the expression level of Skp2 in NSCLC using online databases. Searches in the OncoPrint database, including Hou Lung,<sup>21</sup> Landi Lung,<sup>22</sup> Selamat Lung,<sup>23</sup> and Su Lung,<sup>24</sup> indicated that the Skp2 mRNA level in lung tumors is higher than that in adjacent tissues (Figure 1A). Furthermore, the association between Skp2 expression and NSCLC patients' prognosis was analyzed by Kaplan–Meier plotter (kmplo) (Affymetrix ID: 203626\_s\_at) and prognoscan databases (Data Set: GSE31210). We found that the expression level of Skp2 was negatively associated with patients' prognosis (Figure 1B, C). These results suggested that Skp2 represents a potential therapeutic target in NSCLC.

**FIGURE 1** Online database analyses show that the higher expression of Skp2 is negatively associated with patients' prognosis. A, The expression of Skp2 in the Hou Lung, Landi Lung, Selamat Lung, and Su Lung of OncoPrint datasets is shown. B, The Kaplan–Meier survival curve of non-small cell lung cancer (NSCLC) patients with high or low expression levels of Skp2 is determined by the kmplo database. C, The association between the expression levels of Skp2 and the prognosis of patients is determined by the prognoscan database. \*\**P* < .01, and \*\*\**P* < .001 vs normal group



As phytochemicals display a broad diversity of chemical structures and biological properties, we sought to identify Skp2 inhibitors from a phytochemical library that we had previously established. The crystal structure of Skp2 obtained from the RCSB Protein Data Bank (code: 2AST) served as a query to run our high-throughput structure-based virtual screening (Figure 2A). The potential ligand-binding pocket is comprised of residues L114, E116, L118, W137, L140, L142, K145, L147, H148, V151, R154, L155, and L416, located at the interface of the Skp2-Skp1 interactions, close to the C-terminus and the first leucine-rich repeat of Skp2. This region contributes substantially to the stability of the Skp2-SCF complex.<sup>25</sup> We screened 841 phytochemicals, and 24 hits had the higher predicted binding potential to Skp2 (Figure 2A and Table S1). When docked to Skp2, most compounds directly form one or two H-bonds with the residue R154 or K145. In addition, hydrophobic interactions, Van der Waals interactions, and shape complementarity are major contributors to the binding of Skp2. Considering both commercial availability and the predicted binding affinity, we selected four hits, including camptothecin, procyanidin B1, hesperidin, and BA, for further assessment. First, we tested whether the compounds could block the binding of Skp2 to Skp1 by co-IP. As camptothecin had been pharmacologically characterized, it was used at .5  $\mu\text{mol L}^{-1}$ ; the other three compounds and SZL-P1-41 were used at 30  $\mu\text{mol L}^{-1}$ . We found that both BA and camptothecin drastically prevent the interactions between Skp2 and Skp1, compared with the Skp2 inhibitor SZL-P1-41 (Figure 2B). Because camptothecin is a specific topoisomerase I inhibitor with high toxicity,<sup>26</sup> topoisomerase I inhibition mainly contributes to the cytotoxicity of camptothecin. Meanwhile, BA has shown selective cytotoxicity against cancer cells<sup>27</sup> and its target remains elusive; therefore, we further examined whether BA acts as a potent Skp2 inhibitor.

### 3.2 | Betulinic acid prevents Skp2-Skp1 interaction and inhibits Skp2-SCF E3 ligase activity

To confirm the ability of BA to reduce Skp2-Skp1 interactions, we further performed co-IP experiments to measure the interactions of endogenous proteins in the presence or absence of the inhibitor. These experiments revealed that BA acts as a potent Skp2 inhibitor by preventing Skp2-Skp1 interactions (Figure 2C, D). As Skp2-SCF E3 ligase triggers the ubiquitination and degradation of p27 and E-cadherin, we assessed Skp2-SCF E3 ligase activity by measuring p27 and E-cadherin ubiquitination in the presence or absence of BA. The results revealed that BA markedly inhibited Skp2-mediated endogenous or exogenous ubiquitination of p27 and E-cadherin (Figure 2E-H); BA has a comparable inhibitory effect on p27 ubiquitination to that of SZL-P1-41. CETSA was performed to investigate the direct binding of BA to Skp2. The heat challenge quickly led to Skp2 denaturation and precipitation, while BA significantly increased the thermal stability of Skp2 protein at higher temperatures, demonstrating a direct binding of BA to Skp2 (Figure 2I, J). The above

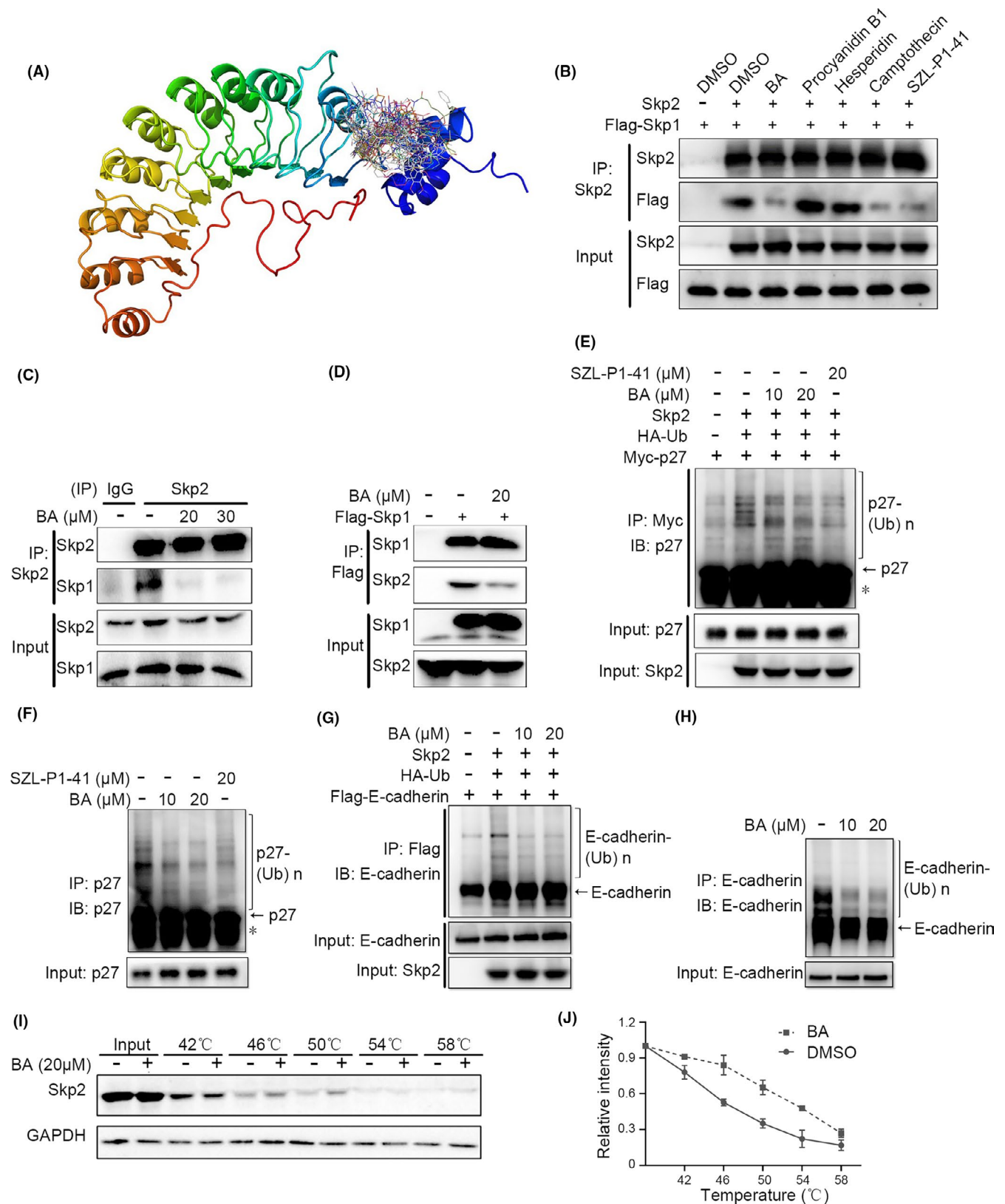
results demonstrate that BA targets Skp2 and inhibits Skp2-SCF E3 ligase activity.

### 3.3 | Betulinic acid directly interacts with Skp2 at the Lys145 residue

To understand how BA interacts with Skp2 and blocks the formation of Skp2-Skp1 complex, we analyzed the molecular docking results and found that H-bonds were formed between BA and the residues Lys145 of Skp2 (Figure 3A, B). To confirm the contribution of the residue to BA binding, the Lys145 of Skp2 was mutated to Ala145 (Skp2 K145A). This mutated protein retained its binding capacity to Skp1 (Figure 3C). However, BA treatment could not significantly prevent the binding of Skp2 K145A to Skp1, compared with its effect on blocking the interaction between Skp2 WT and Skp1 (Figure 3C). Furthermore, CETSA showed that the thermal stability of Skp2 K145A was not significantly affected by BA (Figure 3D, E), confirming that the residue Lys145 is required for the binding of BA to Skp2.

### 3.4 | Betulinic acid induces the accumulation of p27 and E-cadherin in non-small cell lung cancer cells

To determine the effects of BA on the Skp2-SCF E3 ligase-mediated signal pathway, we first tested the cytotoxicity of BA against NSCLC. BA at appropriate concentrations ( $\leq 20 \mu\text{mol L}^{-1}$ ) that could not induce apparent cell death in NSCLC (Figure S1A, B) were utilized for further experiments. As Skp1 stabilizes Skp2 in the SCF complex,<sup>10,28</sup> we examined the effect of BA on Skp2 protein stability by CHX assay. Co-treatment with CHX and BA significantly decreased Skp2 protein stability within 6 hours, compared with CHX treatment alone (Figure 4A, B), suggesting that BA decreases Skp2 protein stability through dissociating Skp2 from the SCF complex. Consistently, BA treatment significantly decreased Skp2 and increased p27 and E-cadherin protein levels in a dose- and time-dependent manner (Figure 4C-H), which was in line with decreased p27 and E-cadherin ubiquitination upon BA treatment (Figure 2E-H). Because previous studies have shown that Skp2 is involved in the epithelial-mesenchymal transition (EMT) occurring in osteosarcoma and breast cancer cells,<sup>29,30</sup> we assessed whether BA would affect other EMT-related proteins. We found that BA only slightly affected the expression of the mesenchymal markers N-cadherin and vimentin at a high dose (Figure 4E). Moreover, the expression of transcriptional repressors of E-cadherin, including Slug, Twist, and Snail, was not obviously affected by BA (Figure S2). As Skp2 is involved in TGF- $\beta$ -induced EMT,<sup>31</sup> we then examined the effects of BA on the TGF- $\beta$ -induced EMT process. As expected, BA treatment significantly attenuated TGF- $\beta$ -induced upregulation of Skp2 and then promoted the accumulation of E-cadherin; BA also suppressed TGF- $\beta$ -induced upregulation of N-cadherin and Vimentin (Figure S3). Taken together, these results indicate that BA can induce the accumulation of Skp2 substrates and potentially inhibit the EMT process in NSCLC.



### 3.5 | Betulinic acid inhibits the migration and stemness in non-small cell lung cancer

Skp2 facilitates cancer metastasis and stemness through promoting the ubiquitination of its substrate proteins.<sup>5</sup> Accordingly, we

tested whether BA could affect migration and stemness in NSCLC. As expected, BA significantly suppressed NSCLC cell migration and invasion in wound-healing and transwell assays (Figure 5A-D). Moreover, BA markedly reduced the sphere-forming potential of NSCLC cells cultured in non-adherent conditions (Figure 5E) or

**FIGURE 2** Identification of betulinic acid (BA) as a Skp2 inhibitor. A, Plant-derived compounds were docked to the binding pocket of Skp2-Skp1. Skp2 and compounds are shown as cartoon and line, respectively. B, Co-immunoprecipitation (co-IP) experiments were performed to examine the effects of four selected compounds and SZL-P1-41 on Skp2-Skp1 binding in 293T cells transfected with Skp2 and Flag-Skp1. C, Endogenous Skp2-Skp1 interactions with or without BA in H1299 cells were examined by co-IP. D, 293T cells were transfected with Flag-Skp1 to examine the Skp2-Skp1 interaction with or without BA treatment. E, Ubiquitination assay of exogenous p27 in 293T cells transfected with Myc-p27, HA-Ub, and Skp2 upon BA or SZL-P1-41 treatment. F, Ubiquitination assay of endogenous p27 in A549 cells upon BA or SZL-P1-41 treatment. The asterisk indicates the bands of IgG light chain. G, Ubiquitination assay of exogenous E-cadherin in 293T cells transfected with Flag-E-cadherin, HA-Ub, and Skp2 upon BA treatment. H, Ubiquitination assay of endogenous E-cadherin in A549 cells upon BA treatment. I, J, A cellular thermal shift assay (CETSA) of Skp2 was conducted by western blotting (I); quantification of the cellular thermal curve shift of Skp2 protein (J)

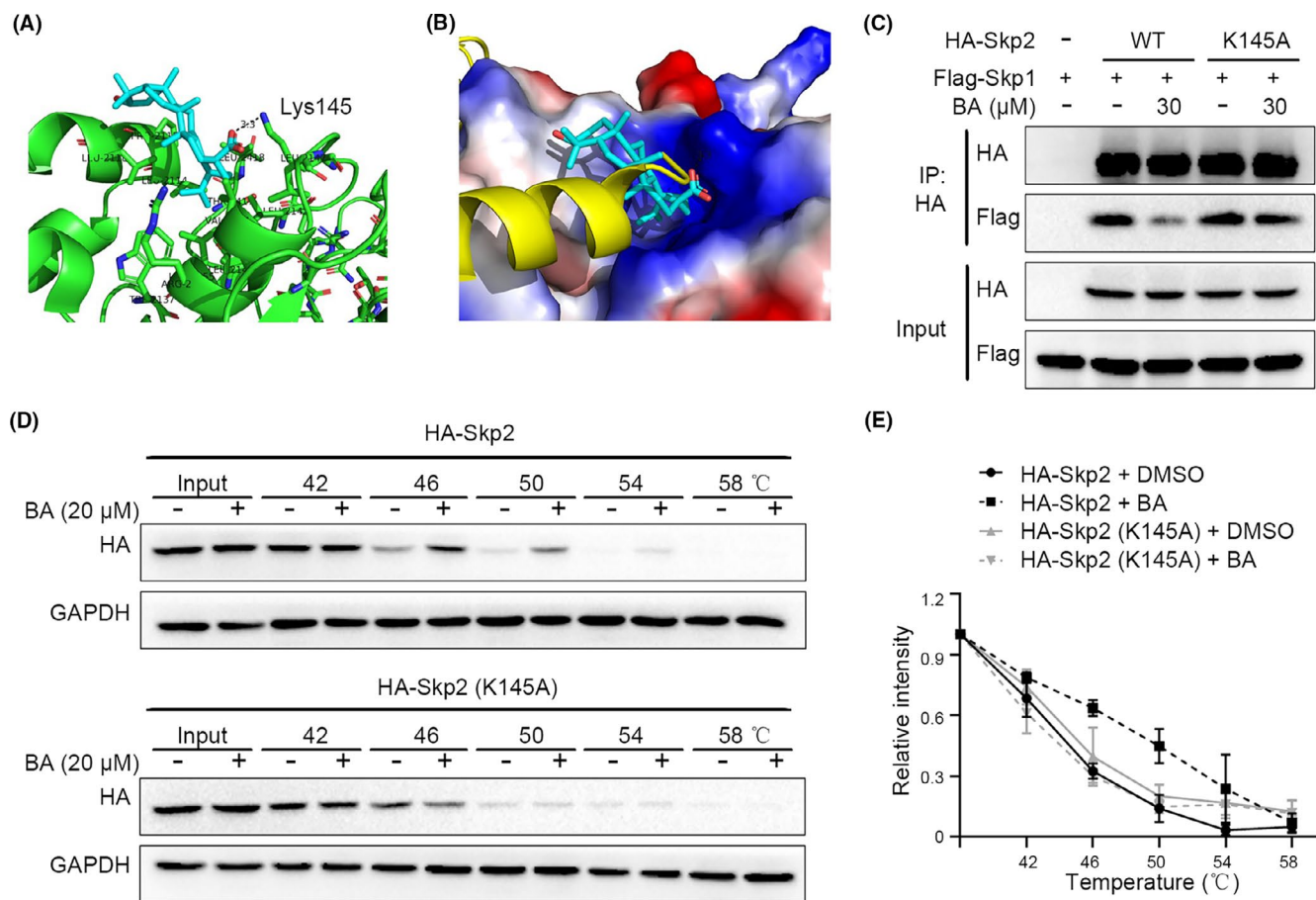


**FIGURE 3** Betulinic acid (BA) directly interacts with Skp2 at Lys145 residue. A, Molecular docking revealed the potential binding residue of BA in Skp2; BA is shown as sticks and the residues composed of the pocket are labeled and shown as lines. B, BA (shown as sticks) was demonstrated to disrupt the interaction of Skp2 (shown as electrostatic potential surface) with Skp1 (shown as cartoon) by docking. C, 293T cells were transfected with Flag-Skp1 and HA-Skp2 WT or HA-Skp2 K145A to perform Skp2-Skp1 binding assay with or without BA treatment for 6 h. D, 293T cells were transfected with HA-Skp2 WT or HA-Skp2 K145A to perform a cellular thermal shift assay (CETSA) with or without BA (20  $\mu$ mol L<sup>-1</sup>) treatment. E, Quantification of the cellular thermal curve shift of Skp2 protein

three-dimensional Matrigel (Figure 5F), as evidenced by smaller and fewer tumor spheres in BA-treated groups. BA also significantly induced cell cycle arrest in G1 phase (Figure S4). These data suggest that besides its capacity to limit NSCLC proliferation, BA can also efficiently inhibit the migratory and stem-like properties of lung cancer cells.

### 3.6 | Overexpression of Skp2 reverses the antimigratory properties of betulinic acid

To examine whether the inhibitory effects of BA on cell migration were linked to its effect on Skp2, we established stable overexpression of Skp2 in two cell lines, H1299 and A549. Skp2

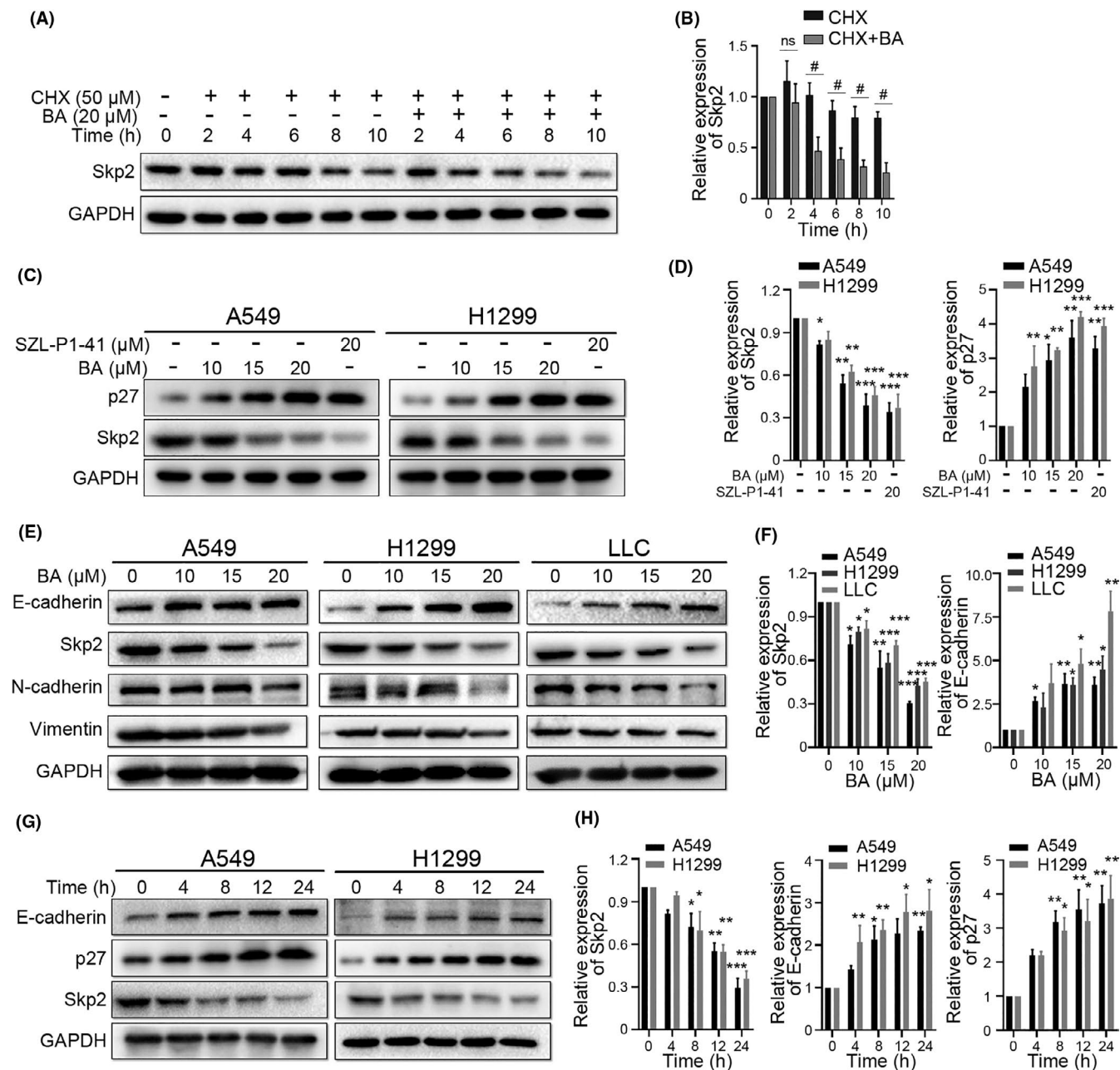


**FIGURE 4** Betulinic acid (BA) decreases Skp2 and increases p27 and E-cadherin in non-small cell lung cancer (NSCLC) cells. A, B H1299 cells were treated with cycloheximide (CHX) in the presence or absence of BA for indicated time; protein levels of Skp2 were detected by western blotting (A); Skp2 protein level was quantified by densitometry analysis (B). C, D The protein levels of Skp2 and p27 in A549 and H1299 cells were examined by western blotting upon BA or SZL-P1-41 treatment for 24 h (C); protein levels of Skp2 and p27 were quantified by densitometry analysis (D). E, F The protein levels of the indicated proteins in H1299, A549, and Lewis lung carcinoma cell line (LLC) cells were examined by western blotting upon BA treatment for 24 h (E); protein levels of Skp2 and E-cadherin were quantified by densitometry analysis (F). G, H The protein levels of Skp2, p27, and E-cadherin were detected by western blotting after BA (20  $\mu$ mol L<sup>-1</sup>) treatment for indicated time points (G); quantification of Skp2, p27, and E-cadherin by densitometry analysis (H). All data are expressed mean  $\pm$  SEM. #*P* < .05 vs BA treatment groups. \**P* < .05, \*\**P* < .01, and \*\*\**P* < .001 vs control

overexpression significantly downregulated E-cadherin protein level (Figure 6A) and was accompanied by enhanced migration and invasion of NSCLC (Figure 6C, E), indicating that Skp2-SCF E3 ligase/E-cadherin axis is essential for the migration and invasion of NSCLC. Upon Skp2 overexpression in NSCLC, the capacity of BA to downregulate Skp2, and thereby to promote

E-cadherin accumulation, was significantly attenuated (Figure 6B). Consistently, overexpression of Skp2 also partially reversed the inhibitory effects of BA on NSCLC migration and invasion (Figure 6C-F). Therefore, our results confirmed that Skp2 is one of the critical targets of BA and is, indeed, involved in BA-mediated inhibition of migration and invasion of NSCLC.



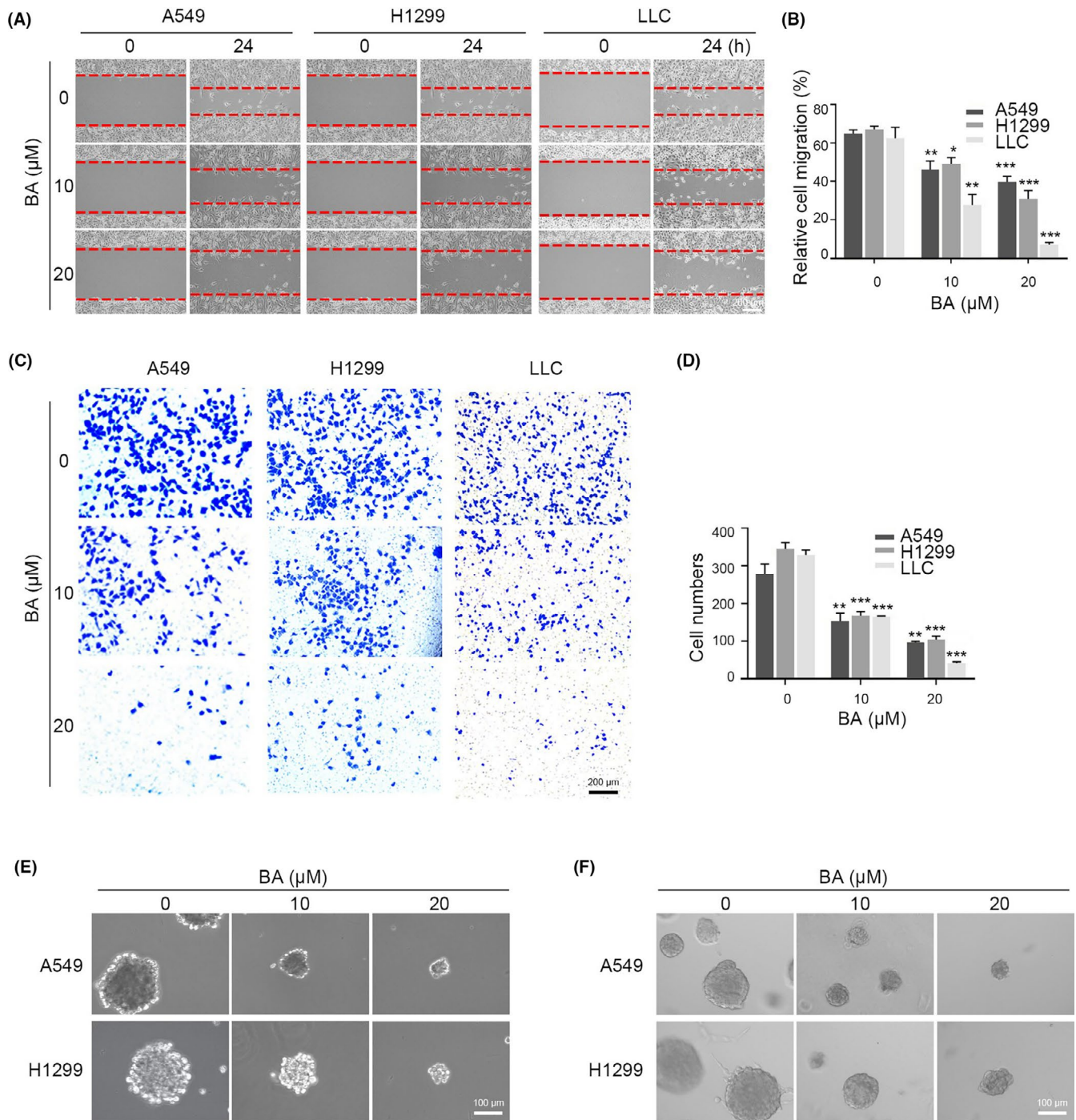


**FIGURE 5** Betulinic acid (BA) inhibits cell migration and stemness of non-small cell lung cancer (NSCLC). A, B Wound healing assay of NSCLC cells treated with BA: cells were imaged and visualized by light microscopy (A); relative migration rate was quantified by ImageJ software (B). C, D Transwell assay of NSCLC cells treated with DMSO or BA (C); cells were counted from three independent experiments (D). E, A549 and H1299 cells cultured in non-adherent conditions were treated with DMSO or BA for 7 days. Spheroids were photographed by light microscopy. F, A549 and H1299 cells cultured in three-dimensional Matrigel were administered with DMSO or BA for 7 days. Images were obtained via optical microscope. The values are expressed as the means  $\pm$  SEM; \* $P < .05$ , \*\* $P < .01$ , and \*\*\* $P < .001$  vs control

### 3.7 | Betulinic acid suppresses tumor growth and metastasis in vivo

Previous studies have demonstrated that BA exhibits antitumor activities without acute or chronic toxicity.<sup>32</sup> To determine the in vivo antimetastatic potential of BA in NSCLC, highly metastatic

LLC cells were used to establish a spontaneous metastasis model in mice. In subcutaneous tumor xenografts, we observed obvious subcutaneous tumor growth that was accompanied by marked tumor metastasis into the lung (Figure 7A-D). However, administration of BA significantly inhibited primary tumor growth (Figure 7A, B), as well as spontaneous lung metastasis (Figure 7C, D), without

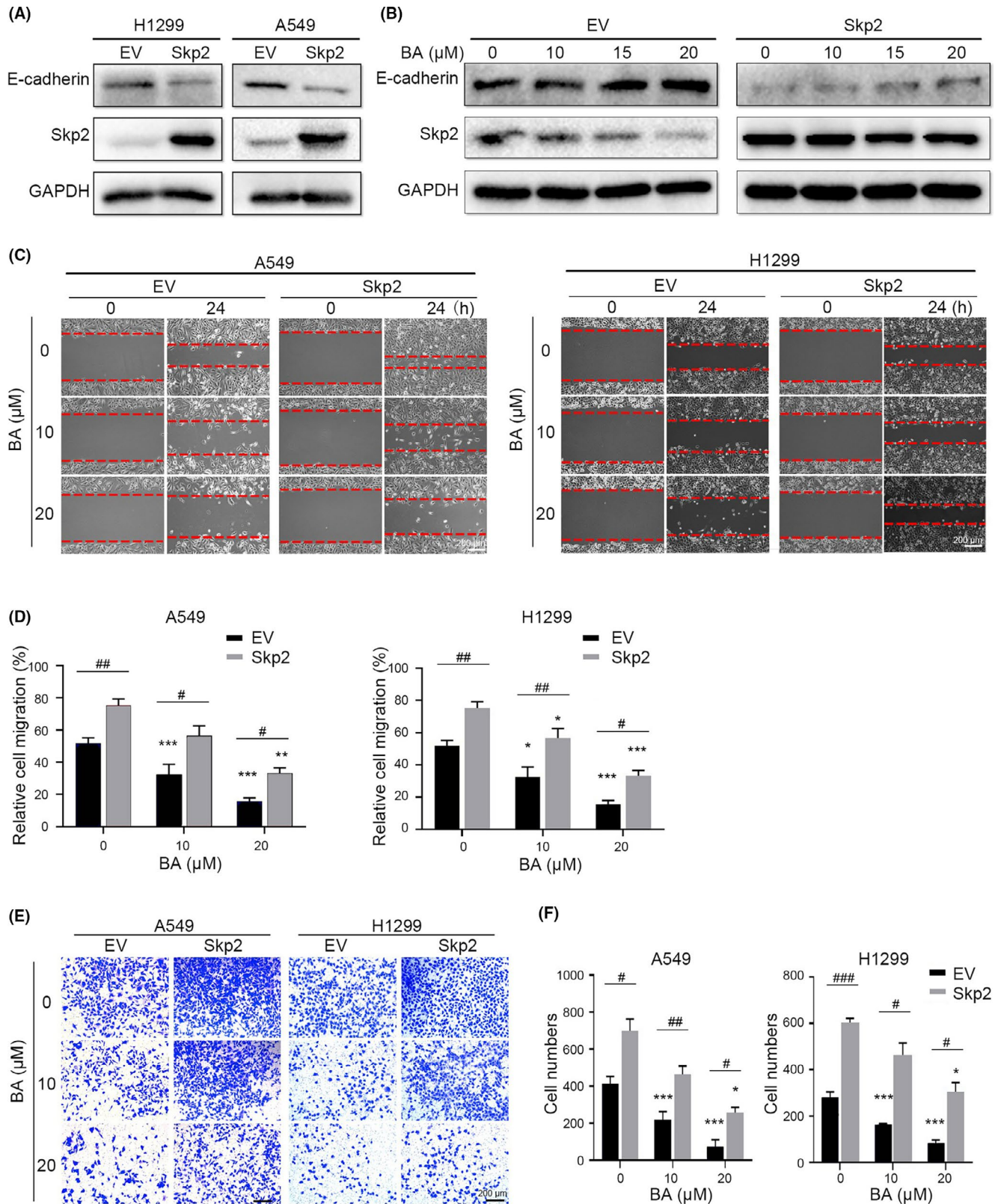


**FIGURE 6** Overexpression of Skp2 reverses the antimigration effect of betulinic acid (BA). A, Protein levels of Skp2 and E-cadherin in non-small cell lung cancer (NSCLC) cells stably overexpressing Skp2 were examined by western blotting. B, H1299 cells with Skp2 overexpression or EV were treated with BA for 24 h; the expression of Skp2 and E-cadherin were examined by western blotting. C, D Wound healing assays of A549 and H1299 cells stably overexpressing Skp2 in the presence or absence of BA (C); relative migration rate was quantified by ImageJ software (D). E, F Transwell assay of A549 and H1299 cells that stably overexpress Skp2 (E); cells were counted from three independent experiments (F). EV, empty vector. The values are expressed as mean  $\pm$  SEM. \* $P < .05$ , \*\* $P < .01$ , and \*\*\* $P < .001$  vs controls. # $P < .05$ , ## $P < .01$ , and ### $P < .001$  vs EV group

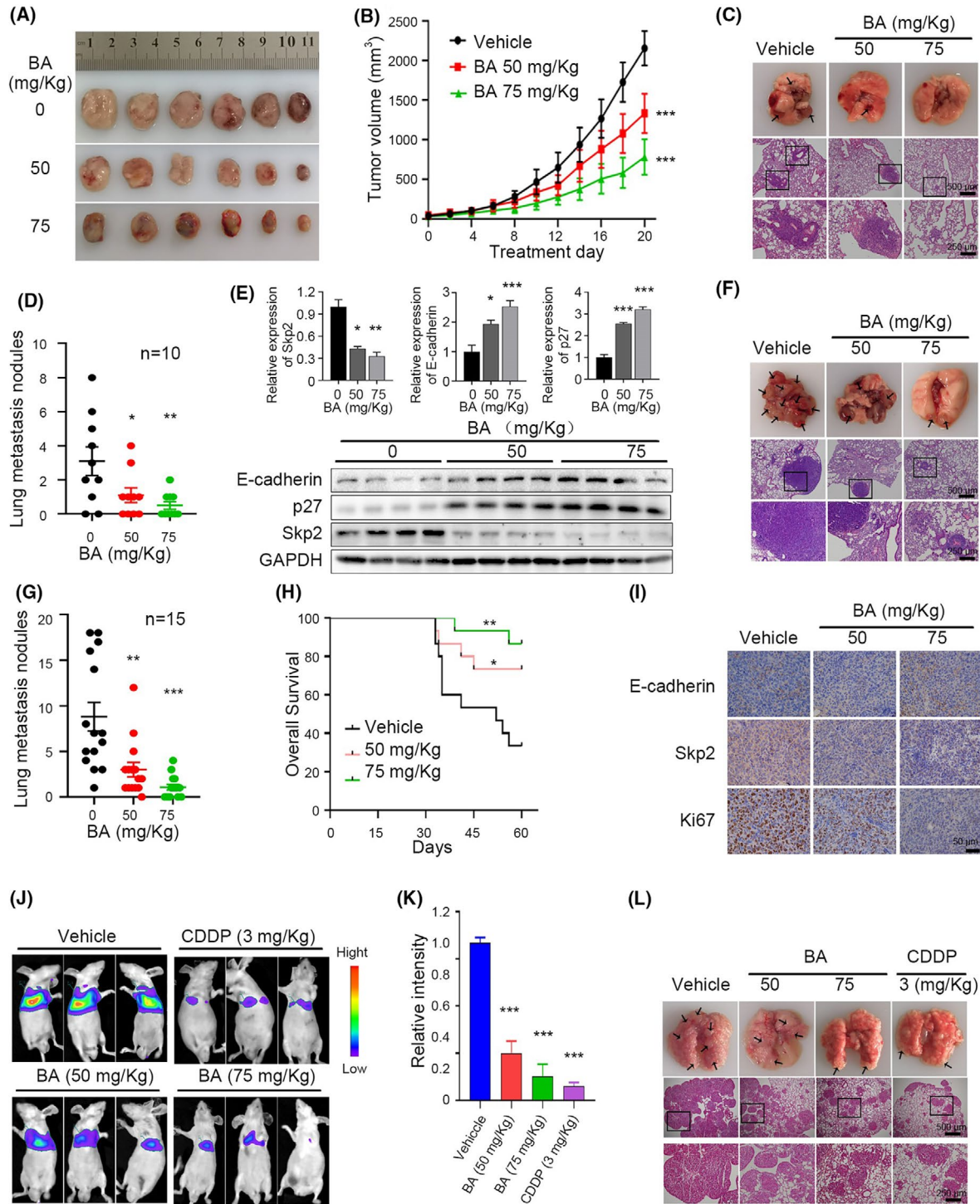


**FIGURE 7** Betulinic acid (BA) suppresses tumor growth and metastasis in vivo. A-E, Images of subcutaneous xenografted tumors of Lewis lung carcinoma cell line (LLC) cells were dissected and photographed A. Tumor volumes were measured and calculated B. Representative pictures of lung metastases (upper panel) and the H&E staining of metastatic nodules (lower panel) in the lung tissue of each group are shown (C). Number of metastasis nodules was counted (D). Protein levels of Skp2, p27, and E-cadherin were detected by western blotting and quantified by densitometry analysis from four mice from each group (E). F-I, LLC cells were injected into C57BL/6 mice via tail vein to establish lung metastasis model. Representative pictures of lung metastases (upper panel) and H&E staining of lung tissue sections (lower panel) are shown (F). The number of metastasis nodules in the lung tissue was counted (G). Overall survival analysis of mice receiving indicated treatments (H). Immunohistochemistry (IHC) analysis of E-cadherin, Skp2, and Ki67 expression in the lung tissues (I). J-L, A549-Luciferase cells were intravenously injected into BALB/C nude mice. Bioluminescence images were obtained (J), and the relative luminescence intensity in the mice was calculated (K). Representative pictures of lung metastases (upper panel) and H&E staining of lung tissue sections (lower panel) of the nude mice (L). Black arrows: metastasis nodules in the lung tissue. The values are expressed as the mean  $\pm$  SEM. \* $P < .05$ , \*\* $P < .01$ , and \*\*\* $P < .001$  vs vehicle control

affecting the body weight of the mice (Figure S4). H&E staining showed that metastatic nodules in BA-treated groups were much smaller than those in the control group (Figure 7C). As expected, BA treatment downregulated Skp2 while upregulating p27 and E-cadherin protein levels in the subcutaneous-xenografted tumor tissues (Figure 7E).

Furthermore, in another experimental setup of lung metastasis established by intravenously injection of LLC cells, BA administration also significantly decreased the number and size of metastatic lung nodules and prolonged the lifespan of the mice (Figure 7F-H). H&E staining confirmed that BA reduced the metastatic tumor burden in lung tissues (Figure 7F). Meanwhile, BA administration decreased Skp2 and increased E-cadherin protein levels, as visualized by IHC staining. Analysis of Ki67 expression indicated that BA also significantly inhibited cell proliferation (Figure 7I).

To extend the applicability of BA to antimetastasis treatment, we further investigated the antimetastatic effect of BA in nude mice that were injected intravenously with A549-luciferase cells. BA treatment markedly suppressed lung A549 metastases, evidenced by decreased bioluminescence intensity and reduced number of pulmonary metastatic foci, without obvious toxicity (Figure 7J-L and Figure S5). In addition, H&E staining showed that BA strongly reduced the size of lung metastatic nodules (Figure 7L). These results demonstrate that BA exhibits a favorable antimetastatic potential via targeting the Skp2-SCF E3 ligase.

## 4 | DISCUSSION

Despite significant advances in NSCLC treatment, metastases remain the leading cause of cancer deaths among NSCLC patients. Targeted therapy has been shown to be effective in the treatment of cancers and to overcome the adverse effects of chemotherapy. However, few drugs have been developed to treat tumor metastasis. Skp2-targeted therapy has emerged as an efficient approach to inhibit the proliferation, metastasis, and stemness of cancer. Multiple chemical probes have been demonstrated to target Skp2 and inhibit Skp2-mediated degradation of p27.<sup>11,33,34</sup> In the present study, we further explored novel Skp2 inhibitors that may qualify as anticancer drug candidates. Based on high-throughput virtual screening, we identified BA as a potent Skp2 inhibitor. BA inhibits Skp2-SCF E3 ligase and induces the accumulation of p27 and E-cadherin, thus inhibiting both proliferation and metastasis of NSCLC. Our results showed that BA exhibits promising therapeutic efficacy to eradicate tumor metastasis in NSCLC.

Plant-derived compounds, which display a broad chemical diversity, constitute a huge library for anticancer drug discovery. To date, ample evidence has demonstrated that natural products harbor great diversity of chemicals that can be screened for novel anticancer agents or lead structures.<sup>35-37</sup> Previously, we have successfully screened novel Skp1 inhibitors from a phytochemical library that contains a broad variety of chemical structures.<sup>7</sup> Here, the phytochemical library was further probed to identify novel Skp2-targeting

inhibitors, and a small compound BA drew our attention. BA has been widely demonstrated to possess a potential antitumor effect with low cytotoxicity towards normal cells.<sup>27,32</sup> BA was first identified as a potential inhibitor of human melanoma without obvious toxicity.<sup>32</sup> Phase 1 clinical trials (NCT00701987 and NCT030904511) have been conducted to evaluate its safety, tolerability, and preliminary efficacy for the treatment of cutaneous metastatic melanoma, supporting its potential application for the treatment of human malignancies.<sup>38</sup> The underlying mechanisms by which BA inhibits tumor growth have been gradually uncovered. BA acts as an SP1 inhibitor and reduces lung cancer cell proliferation.<sup>39</sup> BA can also inhibit cancer metastasis via the downregulation of Lamin B1, MMP-2, MMP-9, and TIMP2.<sup>40,41</sup> However, the underlying mechanism by which BA exerts its antimetastatic effect in NSCLC is unclear. In our study, we found that BA significantly inhibits NSCLC metastasis at subtoxic concentrations. Based on molecular docking and targeted-mutagenesis, we found that BA may bind to residue Lys145 of Skp2 located in the core part of the Skp1-Skp2 interface, and CETSA experiments further demonstrated that BA can bind to Skp2. However, whether BA targets other metastasis-related proteins requires further investigation.

Several studies have revealed the critical role of Skp2 for tumor proliferation and metastasis. Skp2 is overexpressed in various types of cancers and is associated with cancer metastasis.<sup>31,42</sup> It is plausible that Skp2 regulates cell cycle progression through controlling the stability of p27 and p21 proteins.<sup>43,44</sup> In the meantime, several mechanisms have been reported to be involved in the migration-promoting effect of Skp2. Skp2 regulates the expression of migration-related proteins such as MMP2/9, Twist, and RhoA.<sup>45-47</sup> It can also regulate cell migration by promoting the ubiquitination of E-cadherin.<sup>5</sup> Herein, we found that BA significantly increased the expression of E-cadherin. Consistently, Skp2 overexpression markedly decreases the E-cadherin protein level and reverses the inhibitory effect of BA on NSCLC migration. Therefore, our study provides evidence that Skp2-targeting drugs regulate cell migration mainly through controlling the E-cadherin protein level. These data demonstrate the critical role of Skp2-SCF E3 ligase in regulating tumor metastasis.

To date, multiple Skp2 inhibitors have been identified by high-throughput screening, based on the structural properties of Skp2-SCF E3 ligase. Skp2 interacts with Skp1 via its F-box motif and binds its substrates through variable protein interaction domains.<sup>48</sup> The specific binding and ubiquitination of p27 by Skp2 also requires the Cks1 protein.<sup>49</sup> Compounds that attenuate the interaction between Skp2-Cks1 and p27 can specifically inhibit the degradation of p27.<sup>11,50</sup> Meanwhile, compounds such as SZL-P1-41 have been identified to bind to the Skp1-Skp2 interaction interface and dissociate Skp2 from the SCF complex, thus leading to the inhibition of its E3 ligase activity and attenuating the ubiquitination of its diverse substrates.<sup>10</sup> In our study, we aimed to find novel Skp2 inhibitors that can suppress its E3 ligase activity. We identified BA and camptothecin as potential Skp2-SCF E3 ligase inhibitors by preventing Skp2-Skp1 interaction. Camptothecin, a well-known topoisomerase

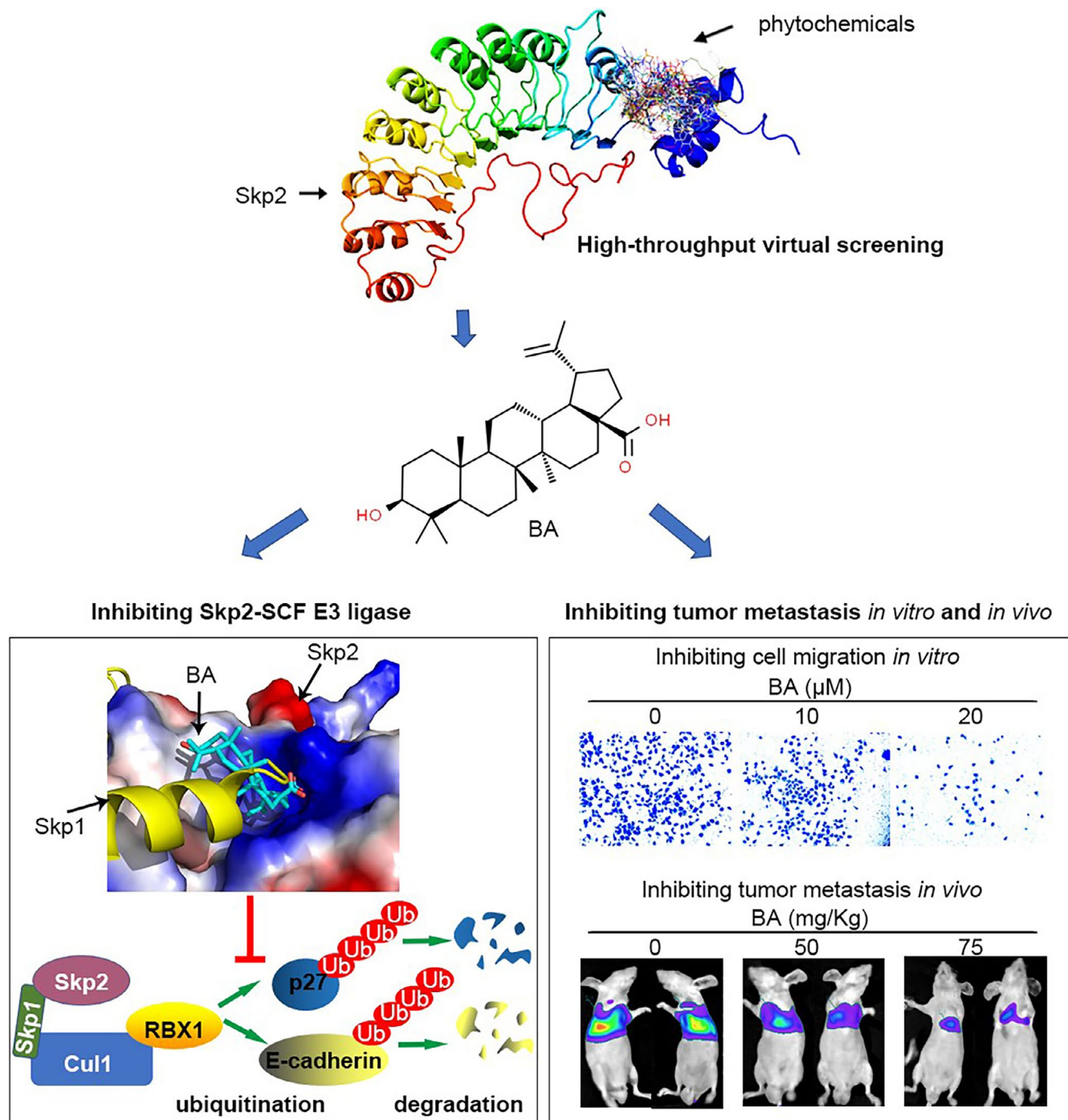


**FIGURE 8** Schematic identification of betulinic acid as a novel Skp2-SCF E3 ligase inhibitor to inhibit proliferation and metastasis of non-small cell lung cancer (NSCLC)

I inhibitor, exhibits high toxicity through inducing DNA damage and cell apoptosis; thus, we examined the inhibitory effect of BA on Skp2-SCF E3 ligase and demonstrated that it exhibited promising therapeutic efficacy through inducing the accumulation of p27 and E-cadherin.

In conclusion, our study demonstrated that BA inhibits proliferation and migration of NSCLC both *in vivo* and *in vitro* by targeting Skp2 and suppressing Skp2-mediated p27 and E-cadherin ubiquitination (Figure 8). Therefore, our study provides novel evidence

supporting the antiproliferative and antimetastatic potential of BA in NSCLC, which is worthy of further clinical investigation.

#### ACKNOWLEDGMENTS

This work was supported by the National Natural Science Foundation of China (81802776, 82004161), Guangzhou Science Technology and Innovation Commission Technology Research Projects (201805010005), and the Project of South Medicine Innovation Team in Modern Agricultural Industry Technology System of

Guangdong Province (2020KJ148). The authors thank Dr Guang-Biao Zhou (State Key Laboratory of Molecular Oncology, National Cancer Center) for sharing the A549-luciferase cell line.

### CONFLICT OF INTEREST

The authors declare that they have no competing interests.

### AUTHOR CONTRIBUTIONS

DHH, YLZ, YZL, MH, and YQL designed the research. DHH, YFC, YLZ, SBZ, SFW, XZF and XJY performed the experiments. DHH, YFC, SFW, MH, and XZF analyzed the data. DHH, YZL, and YQL drafted the manuscript. DHH, QW, YZL, and YQL reviewed the manuscript.

### ORCID

Yong-Qiang Liu  <https://orcid.org/0000-0003-3826-6878>

### REFERENCES

- Bray F, Ferlay J, Soerjomataram I, Siegel RL, Torre LA, Jemal A. Global cancer statistics 2018: GLOBOCAN estimates of incidence and mortality worldwide for 36 cancers in 185 countries. *CA Cancer J Clin*. 2018;68:394-424.
- Arbour KC, Riely GJ. Systemic therapy for locally advanced and metastatic non-small cell lung cancer: a review. *JAMA*. 2019;322:764-774.
- Wang Z, Liu P, Inuzuka H, Wei W. Roles of F-box proteins in cancer. *Nat Rev Cancer*. 2014;14:233-247.
- Nakayama K, Nagahama H, Minamishima YA, et al. Targeted disruption of Skp2 results in accumulation of cyclin E and p27(Kip1), polyploidy and centrosome overduplication. *EMBO J*. 2000;19:2069-2081.
- Inuzuka H, Gao D, Finley LW, et al. Acetylation-dependent regulation of Skp2 function. *Cell*. 2012;150:179-193.
- Skaar JR, Pagan JK, Pagano M. SCF ubiquitin ligase-targeted therapies. *Nat Rev Drug Discov*. 2014;13:889-903.
- Liu YQ, Wang XL, Cheng X, et al. Skp1 in lung cancer: clinical significance and therapeutic efficacy of its small molecule inhibitors. *Oncotarget*. 2015;6:34953-34967.
- Rico-Bautista E, Yang C-C, Lu L, Roth GP, Wolf DA. Chemical genetics approach to restoring p27Kip1 reveals novel compounds with antiproliferative activity in prostate cancer cells. *BMC Biol*. 2010;8:153.
- Chen Q, Xie W, Kuhn DJ, et al. Targeting the p27 E3 ligase SCF(Skp2) results in p27- and Skp2-mediated cell-cycle arrest and activation of autophagy. *Blood*. 2008;111:4690-4699.
- Chan CH, Morrow JK, Li CF, et al. Pharmacological inactivation of Skp2 SCF ubiquitin ligase restricts cancer stem cell traits and cancer progression. *Cell*. 2013;154:556-568.
- Wu L, Grigoryan AV, Li Y, Hao B, Pagano M, Cardozo TJ. Specific small molecule inhibitors of Skp2-mediated p27 degradation. *Chem Biol*. 2012;19:1515-1524.
- Cragg GM, Grothaus PG, Newman DJ. Impact of natural products on developing new anti-cancer agents. *Chem Rev*. 2009;109:3012-3043.
- Singh S, Sharma B, Kanwar SS, Kumar A. Lead phytochemicals for anticancer drug development. *Front Plant Sci*. 2016;7:1667.
- Du L, Liu X, Ren Y, et al. Loss of SIRT4 promotes the self-renewal of breast cancer stem cells. *Theranostics*. 2020;10:9458-9476.
- Bahmad HF, Cheaito K, Chalhoub RM, et al. Sphere-formation assay: three-dimensional in vitro culturing of prostate cancer stem/progenitor sphere-forming cells. *Front Oncol*. 2018;8:347.
- Sanner MF. Python: a programming language for software integration and development. *J Mol Graph Model*. 1999;17:57-61.
- Hu L, Li Z, Cheng J, et al. Crystal structure of TET2-DNA complex: insight into TET-mediated 5mC oxidation. *Cell*. 2013;155:1545-1555.
- Trott O, Olson AJ. AutoDock Vina: improving the speed and accuracy of docking with a new scoring function, efficient optimization, and multithreading. *J Comput Chem*. 2010;31:455-461.
- Jafari R, Almqvist H, Axelsson H, et al. The cellular thermal shift assay for evaluating drug target interactions in cells. *Nat Protoc*. 2014;9:2100-2122.
- Yagishita S. Co-immunoprecipitation assay to investigate the interaction strength between synaptic proteins using COS-7 cells. In: *Co-Immunoprecipitation Methods for Brain Tissue*. 2019;89-96.
- Hou J, Aerts J, den Hamer B, et al. Gene expression-based classification of non-small cell lung carcinomas and survival prediction. *PLoS ONE*. 2010;5:e10312.
- Landi MT, Dracheva T, Rotunno M, et al. Gene expression signature of cigarette smoking and its role in lung adenocarcinoma development and survival. *PLoS ONE*. 2008;3:e1651.
- Selamat SA, Chung BS, Girard L, et al. Genome-scale analysis of DNA methylation in lung adenocarcinoma and integration with mRNA expression. *Genome Res*. 2012;22:1197-1211.
- Su LJ, Chang CW, Wu YC, et al. Selection of DDX5 as a novel internal control for Q-RT-PCR from microarray data using a block bootstrap re-sampling scheme. *BMC Genom*. 2007;8:140.
- Schulman BA, Carrano AC, Jeffrey PD, et al. Insights into SCF ubiquitin ligases from the structure of the Skp1-Skp2 complex. *Nature*. 2000;408:381-386.
- Slichenmyer WJ, Rowinsky EK, Donehower RC, Kaufmann SH. The current status of camptothecin analogues as antitumor agents. *J Natl Cancer Inst*. 1993;85:271-291.
- Zuco V, Supino R, Righetti SC, et al. Selective cytotoxicity of betulinic acid on tumor cell lines, but not on normal cells. *Cancer Lett*. 2002;175:17-25.
- Yoshida Y, Murakami A, Tanaka K. Skp1 stabilizes the conformation of F-box proteins. *Biochem Biophys Res Commun*. 2011;410:24-28.
- Ding L, Wang C, Cui Y, et al. S-phase kinase-associated protein 2 is involved in epithelial-mesenchymal transition in methotrexate-resistant osteosarcoma cells. *Int J Oncol*. 2018;52:1841-1852.
- Yang Q, Huang J, Wu Q, et al. Acquisition of epithelial-mesenchymal transition is associated with Skp2 expression in paclitaxel-resistant breast cancer cells. *Br J Cancer*. 2014;110:1958-1967.
- Qu X, Shen L, Zheng Y, et al. A signal transduction pathway from TGF-beta1 to SKP2 via Akt1 and c-Myc and its correlation with progression in human melanoma. *J Invest Dermatol*. 2014;134:159-167.
- Pisha E, Chai H, Lee IS, et al. Discovery of betulinic acid as a selective inhibitor of human melanoma that functions by induction of apoptosis. *Nat Med*. 1995;1:1046-1051.
- Lough L, Sherman D, Ni E, Young LM, Hao B, Cardozo T. Chemical probes of Skp2-mediated p27 ubiquitylation and degradation. *Medchemcomm*. 2018;9:1093-1104.
- Malek E, Abdel-Malek MA, Jagannathan S, et al. Pharmacogenomics and chemical library screens reveal a novel SCF(SKP2) inhibitor that overcomes Bortezomib resistance in multiple myeloma. *Leukemia*. 2017;31:645-653.
- Lagunin AA, Goel RK, Gawande DY, et al. Chemo- and bioinformatics resources for in silico drug discovery from medicinal plants beyond their traditional use: a critical review. *Nat Prod Rep*. 2014;31:1585-1611.
- Pye CR, Bertin MJ, Lokey RS, Gerwick WH, Lington RG. Retrospective analysis of natural products provides insights for future discovery trends. *Proc Natl Acad Sci USA*. 2017;114:5601-5606.
- Newman DJ, Cragg GM. Natural products as sources of new drugs from 1981 to 2014. *J Nat Prod*. 2016;79(3):629-661.

38. Ali-Seyed M, Jantan I, Vijayaraghavan K, Bukhari SN. Betulinic acid: recent advances in chemical modifications, effective delivery, and molecular mechanisms of a promising anticancer therapy. *Chem Biol Drug Des.* 2016;87:517-536.
39. Hsu TI, Wang MC, Chen SY, et al. Betulinic acid decreases specificity protein 1 (Sp1) level via increasing the sumoylation of sp1 to inhibit lung cancer growth. *Mol Pharmacol.* 2012;82:1115-1128.
40. Li L, Du Y, Kong X, et al. Lamin B1 is a novel therapeutic target of betulinic acid in pancreatic cancer. *Clin Cancer Res.* 2013;19:4651-4661.
41. Wang W, Wang Y, Liu M, et al. Betulinic acid induces apoptosis and suppresses metastasis in hepatocellular carcinoma cell lines in vitro and in vivo. *J Cell Mol Med.* 2019;23:586-595.
42. Su J, Zhou X, Wang L, Yin X, Wang Z. Curcumin inhibits cell growth and invasion and induces apoptosis through down-regulation of Skp2 in pancreatic cancer cells. *Am J Cancer Res.* 2016;6:1949-1962.
43. Wei W, Ayad NG, Wan Y, Zhang GJ, Kirschner MW, Kaelin WG Jr. Degradation of the SCF component Skp2 in cell-cycle phase G1 by the anaphase-promoting complex. *Nature.* 2004;428:194-198.
44. Asmamaw MD, Liu Y, Zheng YC, Shi XJ, Liu HM. Skp2 in the ubiquitin-proteasome system: a comprehensive review. *Med Res Rev.* 2020;40:1920-1949.
45. Ruan D, He J, Li CF, et al. Skp2 deficiency restricts the progression and stem cell features of castration-resistant prostate cancer by destabilizing twist. *Oncogene.* 2017;36:4299-4310.
46. Yang LJ, Chen Y, Ma Q, et al. Effect of betulinic acid on the regulation of Hiwi and cyclin B1 in human gastric adenocarcinoma AGS cells. *Acta Pharmacol Sin.* 2010;31:66-72.
47. Hung WC, Tseng WL, Shiea J, Chang HC. Skp2 overexpression increases the expression of MMP-2 and MMP-9 and invasion of lung cancer cells. *Cancer Lett.* 2010;288:156-161.
48. Zheng N, Schulman BA, Song L, et al. Structure of the Cul1-Rbx1-Skp1-F boxSkp2 SCF ubiquitin ligase complex. *Nature.* 2002;416:703-709.
49. Ganoth D, Bornstein G, Ko TK, et al. The cell-cycle regulatory protein Cks1 is required for SCF(Skp2)-mediated ubiquitinylation of p27. *Nat Cell Biol.* 2001;3:321-324.
50. Ooi LC, Watanabe N, Futamura Y, Sulaiman SF, Darah I, Osada H. Identification of small molecule inhibitors of p27(Kip1) ubiquitination by high-throughput screening. *Cancer Sci.* 2013;104:1461-1467.

#### SUPPORTING INFORMATION

Additional supporting information may be found online in the Supporting Information section.

**How to cite this article:** He D-H, Chen Y-F, Zhou Y-L, et al. Phytochemical library screening reveals betulinic acid as a novel Skp2-SCF E3 ligase inhibitor in non-small cell lung cancer. *Cancer Sci.* 2021;112:3218-3232. <https://doi.org/10.1111/cas.15005>